A new method for ecological surveying of the abyss using autonomous underwater vehicle photography

Kirsty J. Morris[1]*, Brian J. Bett[1], Jennifer M. Durden[2], Veerle A. I. Huvenne[1]; Rosanna Milligan[3];Daniel O. B. Jones[1], Stephen McPhail[1], Katleen Robert[2], David M. Bailey[3], and Henry A. Ruhl[1]

[1]National Oceanography Centre, University of Southampton Waterfront Campus, European Way, Southampton SO14 3ZH, UK
[2]Ocean and Earth Science, University of Southampton, Waterfront Campus, National Oceanography Centre, University of Southampton Waterfront Campus, European Way, Southampton SO14 3ZH, UK
[3]Institute for Biodiversity, Animal Health and Comparative Medicine, University of Glasgow, Glasgow G12 8QQ, UK

Abstract

The extent and speed of marine environmental mapping is increasing quickly with technological advances, particularly with optical imaging from autonomous underwater vehicles (AUVs). This contribution describes a new deep-sea digital still camera system that takes high-frequency (>1 Hz) color photographs of the seafloor, suitable for detailed biological and habitat assessment, and the means of efficient processing of this mass imagery, to allow assessment across a wide range of spatial scales from that of individual megabenthic organisms to landscape scales (>100 km²). As part of the Autonomous Ecological Surveying of the Abyss (AESA) project, the AUV Autosub6000 obtained > 150,000 seafloor images (~160 km total transect length) to investigate the distribution of megafauna on the Porcupine Abyssal Plain (4850 m; NE Atlantic). An automated workflow for image processing was developed that corrected nonuniform illumination and color, geo-referenced the photographs, and produced 10-image mosaics ('tiles,' each representing a continuous strip of 15-20 m² of seafloor), with overlap between consecutive images removed. These tiles were then manually annotated to generate biological data. This method was highly advantageous compared with alternative techniques, greatly increasing the rate of image acquisition and providing a 10-50 fold increase in accuracy in comparison to trawling. The method also offers more precise density and biodiversity estimates [Coefficient of variation (CV) < 10%] than alternative techniques, with a 2-fold improvement in density estimate precision compared with the WASP towed camera system. Ultimately, this novel system is expected to make valuable contributions to understanding human impact in the deep ocean.

The continued evolution of deep-diving autonomous underwater vehicle (AUV) technology is making the world's oceans more accessible. Despite being the Earth's largest habitat, the deep sea is relatively understudied (Tyler 2003; Glover et al. 2010). It was not until the 1960s and 1970s that the deep sea was appreciated to contain diverse habitats and fauna with a multitude of abyssal hills and seamounts emerging from abyssal plains (Ramirez-Llodra et al. 2011). Relationships between this biological diversity and environmental factors have a poorly understood dependence on analytical scale (Chase and Knight 2013). Only by gathering data across scales in the range of 1 m² to 100 km², often referred to as a landscape scale (Forman 1983), can a greater understanding of the functional relationships and heterogeneity within and between habitats be attempted. Such knowledge is now critical to our ability to manage and conserve deep-sea environments (Ruhl et al. 2011).

Current methods for the study of deep-sea megafauna include trawl sampling and photographic and video surveys. Trawls have been useful in determining some long-term and large-scale patterns in invertebrate and fish ecology (Billett et al. 2001; Haedrich and Merrett 1988). However, each trawl amalgamates specimens collected over its entire length into a single sample, limiting spatial interpretation, and it is often difficult to quantify the true seafloor area sampled. Furthermore, trawls may disturb the habitat under study, and the resultant samples are often damaged with soft-bodied organisms in poor condition or lost. Evidence from time-lapse photography suggests that trawls substantially underrepresent some fauna, particularly the smaller size classes (Bett et al. 2001).

There has been an increased use of image data for marine ecological surveys, both for faunal surveys, measurements of animal activity, and the study of particulate organic matter supply to the seafloor (Bett et al. 2001; Heger et al. 2008; Morris et al. 2012, 2013; Smith et al. 2013). Non-bottom contact photographic methods have the ability to cover a large seafloor area with little environmental impact. They allow fauna that are often poorly represented by other sampling methods to be observed and identified (Rice et al. 1982), and can allow local environmental data to be recorded such as habitat and resource availability (Svoboda 1985; Bett et al. 1995). Quantitative and spatially explicit data can be collected over moderate to very large areas at a definable resolution.

Off-bottom towed cameras, such as the NOC Wide Angle Seabed Photography (WASP; Jones et al. 2009) system, provide within-transect spatial data. However, there are difficulties with controlling the position, altitude, and speed of the camera as it is tethered to the surface vessel and so is influenced by swell. This can lead to a large proportion of photographs being unsuitable for quantitative analysis (Jones et al. 2007). On-bottom towed camera sleds do have better stability, but may be more destructive of the seabed habitat and can have image quality issues from induced turbidity (Wakefield and Genin 1987).

Remotely operated vehicles (ROVs) and human occupied vehicles (HOVs) have also been used to collect photographic and video data, allowing topographically complex habitats to be studied, including deep-sea vent and cold-water coral sites (Morris et al. 2012, 2013; Wheeler et al. 2013). These vehicles may also permit the collection of voucher specimens for identification. However, they have drawbacks for large-scale surveying such as slow transect speeds and large amounts of ship time being required for their operation, as well as the influence of swell, and difficulty holding a constant depth due to the tether connection to the surface vessel and limited thruster power. Both can also induce major fish disturbance from hydraulic noise and continuous flood lighting, leading to systematic error in density estimates (e.g., Stoner et al. 2008).

In contrast, AUVs provide stable imaging platforms that can be operated close to the seafloor in suitable areas, produce less noise than ROVs or HOVs, and do not require continuous lighting. They are capable of sustained operations where the surface vessel is engaged in other work, reducing the ship time dedicated to their operation. It has been long expected that use of AUVs would rapidly increase our knowledge of the distribution of visible megafauna at landscape scales (Forman and Gordon 1986).

Here we describe the implementation of ecological mapping using the NOC Autosub6000 AUV over the Porcupine Abyssal Plain (Fig. 1). With a 6000 m depth capability and a range of 150+ km, this AUV is well suited to landscape-scale ecological surveys in the abyss. We use photographic, geo-location, and geophysical technologies to collect a large quantity of environmental and biological data over an extended area. We present a new method of creating continuous geo-referenced image tiles of the seafloor, which are used to assess faunal density and diversity. Specifically, we focus on methods associated with a downward looking (vertical) camera, discussing these methods and evaluating biological results against data collected by other techniques.

Materials and procedures

Area of investigation

The Porcupine Abyssal Plain (PAP) (Fig. 1) is one of only two abyssal locations worldwide with a long-term (20+ years) time series of benthic biological observations (Hartman et al. 2010). Previous work has concentrated on the link between particulate organic carbon (POC) supply and the response of various elements of the benthic community (Hartman et al. 2010; Kalogeropoulou et al. 2010; Soto et al. 2010). The first intensive benthic program began at PAP in 1989 (Rice 1990). Since then, benthic megafauna data have been primarily collected using trawls and time-lapse photography (Bett et al. 2001; Billett et al. 2010). The trawl data from these previous expeditions provided a taxonomic inventory with which to compare the in situ specimen photographs of this study.

Platform and sensors

Autosub6000 is an autonomous underwater vehicle measuring 5.5 m in length and 0.9 m in diameter, having a weight in air of 1800 kg (Fig. 2). Fitted with lithium polymer rechargeable batteries, it can operate for ~48 h at a speed of 1.7 ms⁻¹. It has an IXSEA Photonic Inertial Navigation System (PHINS) and an RDI Teledyne Workhorse Navigator Acoustic Doppler Current Profiler (ADCP) to enable underwater navigation. A Tritech SeaKing scanning sonar is employed for obstacle avoidance. Two-way communications with the vehicle are achieved via a LinkQuest Tracklink 10000 ultra-short baseline (USBL) system. At the surface communication is possible via a WiFi radio link.

As deployed in the present study, the vehicle carried a sensor suite including dual conductivity, temperature, and depth (CTD) system, optical backscatter-based turbidity sensor, tri-axial magnetometer, 300 kHz ADCP, sidescan sonar; sub-bottom profiler, and multibeam echosounder. In addition to these standard sensors, two cameras (one vertical downward-facing and one oblique forward-facing) were also fitted. Point Gray Research Inc. Grasshopper 2 cameras were employed, with a 2/3-inch sensor (2448 × 2048 pixels, i.e., 5 Mega-pixel). A 12 mm focal length lens with horizontal and vertical acceptance angles 26.71° and 22.65°, respectively, was used. The vertical camera was mounted at 90° to the long-axis of the vehicle in its forward section (Fig. 3). The oblique camera was mounted in the nose of the vehicle, and aimed 35° below the long-axis (Fig. 3). At a target altitude of 3.2 m, the vertical camera captures an image of 2.4 m² of seabed, with the oblique camera imaging an area of approximately 16.5 m².

A NOC-designed xenon strobe unit was used with each camera (11 J, with 2 Hz potential repetition rate). A PC104-
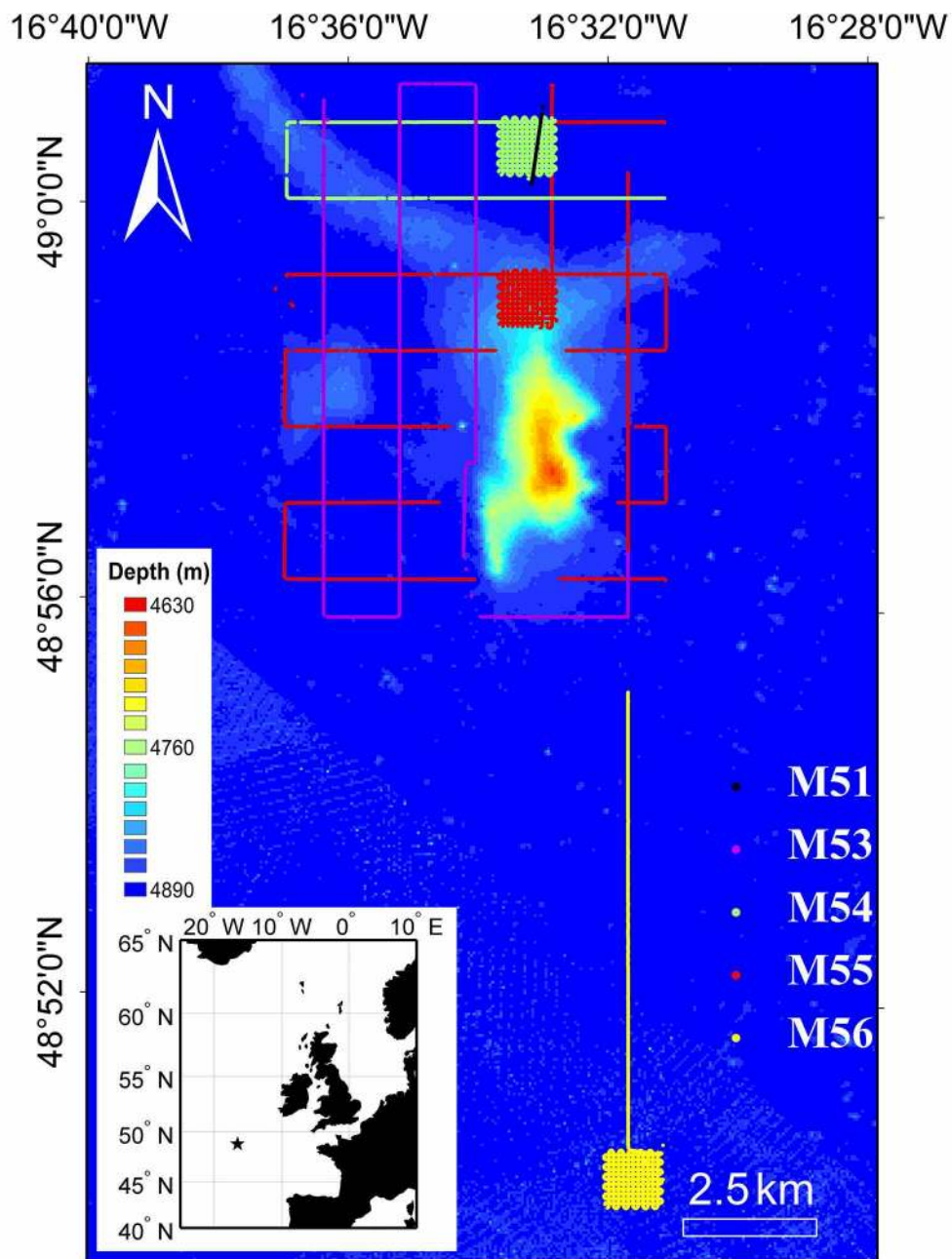
Fig. 1. The study location in the Porcupine Abyssal Plain sustained observatory (PAP-SO) area of the NE Atlantic Ocean off Western Europe (marked by a star on insert map). The main chart shows bathymetry from ship-borne systems at 60 by 60 m pixel resolution with depth color coded according to the scale shown. Coarse scale and fine scale survey grids are shown over an abyssal hill. Mission 56 (yellow line) was ca. 15 km to the south on a flat area of the Abyssal Plain. Colored traces represent individual images taken throughout each given mission between 1.9 and 4.1 m altitude.

based data logger stored engineering data (navigation processor, control sensors, actuation systems) and lower-rate science data (CTD), which was downloaded post-mission via WiFi. High-rate sensors (multibeam, sidescan sonar, sub-bottom profiler, cameras) had their own integral hard drives, accessible over Ethernet (and WiFi). Transfer of large numbers of photographs was most effectively achieved via cabled transfer from the hard drive at the end of each mission. Engineering,

navigation, and science data (e.g., CTD) were recorded at 2-s intervals. These data were then interpolated to provide water depth, altitude, heading, pitch, roll, and geo-location for each seafloor image (0.87 s camera repetition rate). The time period for which the camera took images was determined by considering the nominal velocity of the AUV over the seafloor, the degree of overlap required for tiling, the angular view, and camera resolution, as well as the target altitude for the camera
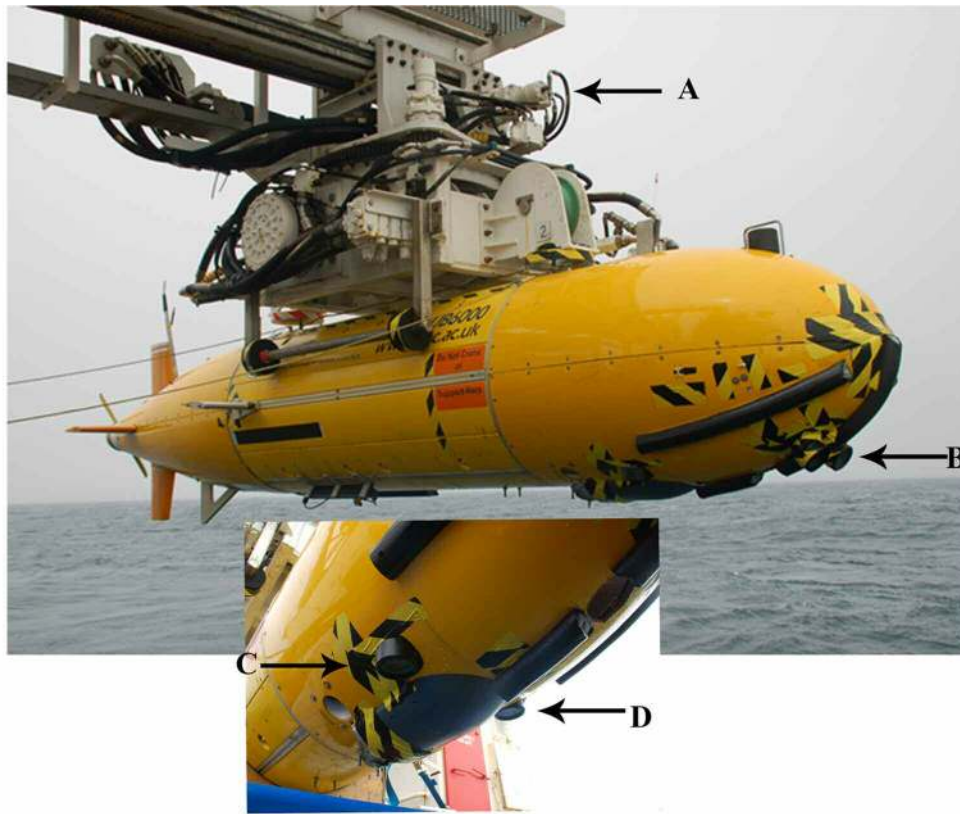
Fig. 2. Autonomous Underwater Vehicle Autosub6000. Here the vehicle is pictured on a gantry (A) following recovery, with the oblique camera and flash visible (B). The inset image shows a zoomed in picture of the vertical camera(C) and flash position (D) on the vehicle.
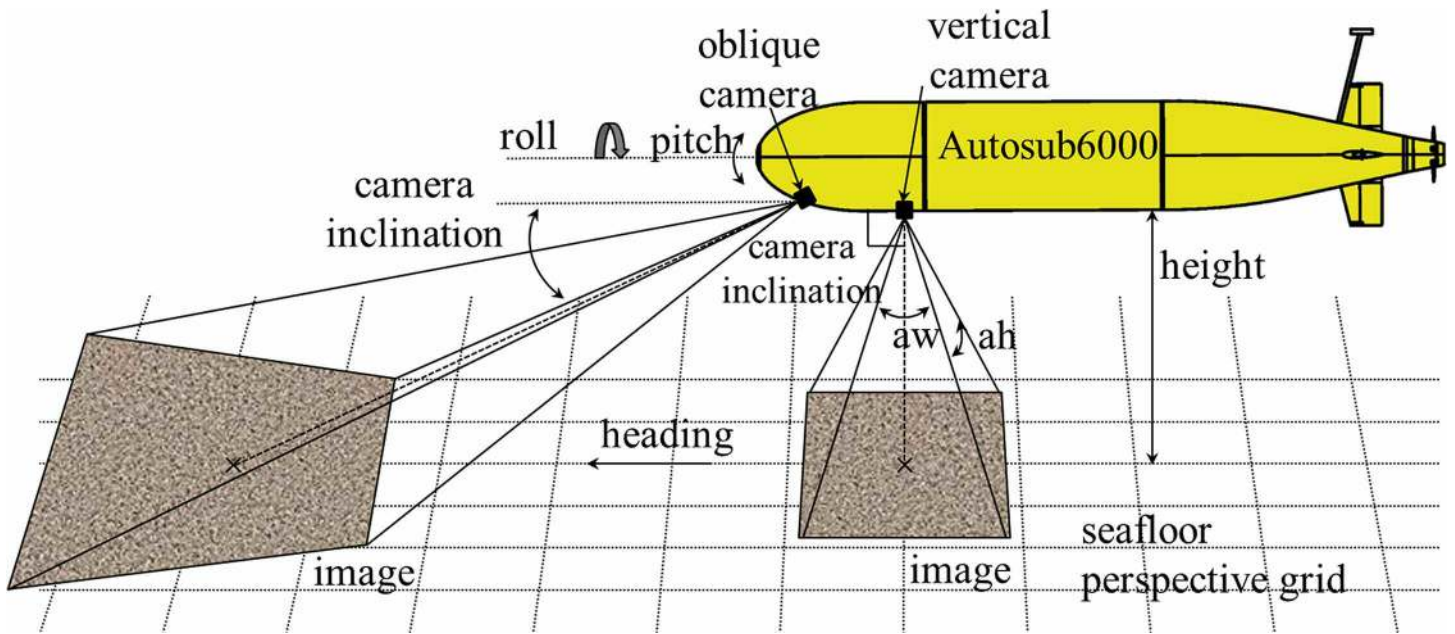
Fig. 3. Schematic of the Autosub6000 in operational mode above the sea floor showing the camera locations and fields of view. aw = angle width; ah = angle height of vertical camera. Note. Autosub and the perspective grid are not to scale.

(which was set at 3.2 following trials during mission 51) for optimal visibility of the seafloor as well as possible identification of smaller animals. The image interval and altitude can be changed dependent on the required outcomes of the missions.

Field operations were carried out in the vicinity of the PAP site (4850 m water depth; 48°50′ N 016°30′ W; Hartman et al. 2012) during RRS *Discovery* cruise 377 (July 2012) (Ruhl 2013). Autosub6000 missions were primarily focused around an abyssal hill located c. 15 km NNW of the PAP central benthic sampling location. Five successful photographic survey missions were carried out during the cruise. General mission deployment operations were as follows: Once in the water, the vehicle acquired a GPS location fix at the surface and a command to initiate the mission was sent to the vehicle via WiFi. The vehicle then dived and began a helical descent to the target altitude. The acoustic modem was used to transfer engineering data to allow monitoring of the operation. When within c. 100 m of the seafloor the Doppler Velocity Log (DVL) became effective in tracking the AUV relative to the seafloor. Both the DVL and the inertial navigation data were combined to give the location of the vehicle. To adjust for any navigational offset accrued during the descent phase, the vehicle started the survey with a navigation box with 1 km sides. The position of the vehicle was monitored from the surface vessel via the USBL system, and any offset from the intended location of the navigation box was calculated and transmitted to the AUV (McPhail and Pebody 2009). The vehicle then updated its absolute geo-location before commencing the science mission.

Mapping survey

Shipborne multibeam swath bathymetry data for the study area acquired on previous surveys [RRS *James Cook* cruises 062 (July/August 2011) and 071 (May 2012); Simrad EM120; Ruhl 2012, 2013] were used for initial AUV mission planning purposes (Fig. 1). Autosub6000 was used to collect additional high resolution bathymetric data (gridded at 5 m × 5 m pixel resolution) over the abyssal hill region of the study area from 100 m altitude. The AUV bathymetry data were collected with a Simrad EM2000 multibeam echosounder (111 beams with a 0.5° roll correction). The AUV position was recorded using range-only navigation algorithms and the inertial navigation output (McPhail 2009). The final map was created within the Caris HIPS and SIPS software, using a BASE (Bathymetric Associated with Statistical Error) surface over a 5 m grid and was used to help determine photographic survey waypoints.

Photographic survey

Two physical scales of observation were assessed during five AUV photographic missions (M51, M53, M54, M55, M56): (i) 'Broad-scale grid' 10 km × 10 km, with 1 km track spacing; and (ii) 'Fine-scale grid' 1 km × 1 km, with 100 m track spacing (Fig. 1). The broad-scale survey encompassed the majority of the abyssal hill and included adjacent areas of level-bottom abyssal plain. Two fine-scale surveys were carried out within the broad-scale survey area, one on the adjacent abyssal plain,

and one on the elevated topography of the abyssal hill (M54 and M55). A third fine-scale survey was carried out in the level-bottom abyssal plain environment of the PAP central area (Billett et al. 2010) 15 km to the south (M56). An additional single photographic survey line was also run between PAP central and the broad-scale survey grid. For all photographic surveys reported here, the target altitude was 3.2 m above the seafloor, and images were recorded every 0.87 s. Here we focus on the vertical downward-facing camera.

Image processing

Autosub6000 completed a total photographic track length of approximately 160 km during the five missions. Following initial inspection, only images from linear track segments (e.g., vehicle turns excluded) where the vehicle altitude was between 1.9 and 4.1 m were processed further (>150,000 images; Table 1). These images were subject to manipulation implemented via a MatlabV2013a (Mathworks) script as below (Web Appendix A).

Dark frame removal

Fifty images from an altitude of 15-30 m were selected, representing control images without seafloor image data. The mean pixel value was calculated to derive an average 'black frame' image and thus the mean level of 'noise,' observed within the images. This black frame image was subtracted from each seafloor image before further processing (Fig. 4a and 4b). This was repeated for each mission.

Nonuniform illumination correction

Fifty seafloor images (1.9-4.1 m altitude) were selected at random within a given mission. For each pixel position in the image the mean intensity was calculated. The mean intensity value was then used to equalize each image in an attempt to minimize illumination vignetting (a reduction in image brightness or saturation at the periphery) before analysis (Fig. 4c).

Color correction

The light path (from flash to seafloor to image sensor) for each image pixel was calculated from the vehicle altitude, assuming the sensor plane was parallel to the seafloor. Individual pixels in the red, green, and blue channels were corrected for percentage light loss assuming the clear type I (oceanic) light attenuation values given by Chiang and Chen (2012) (Fig. 4d).

Geo-referencing

Interpolated latitude and longitude (WGS84) values from the vehicle's navigation record were assigned to the center of each image. To allow the area of the images to be calculated a conversion to the Universal Transverse Mercator (UTM) projected coordinate system (zone 28N) was undertaken. A three-dimensional rotation was then applied to correct for vehicle heading, pitch, and roll. The image was then reprojected to seabed level (Fig. 4d), and in the corresponding seafloor dimensions and geographic position were obtained.

To facilitate subsequent tiling (mosaicking), each image was resampled to a fixed pixel seabed resolution (0.59 mm), equivalent to that of a photograph taken from an altitude of 3 m.

Table 1. Autosub6000 AUV mission data for RRS *Discovery* cruise 377, the Porcupine Abyssal Plain July 2012.

Mission* Q7	Date (2012)	Launch†	Recover‡	Survey time (h)§	Ship time|	Total nr photos	Photos excluding turns	Nr "useful" photos	% useful of total	% useful photos excluding turns
51¶	14 Jul	18:48	09:05	0.30	4.49	1551	1551	880	56.7	56.7
53	17 Jul	19:22	09:32	8.40	4.70	34,988	32,856	31,070	88.8	94.6
54	19 Jul	00:16	14:05	9.11	4.14	37,769	35,018	34,120	90.3	97.4
55	20 Jul	22:42	23:19	19.99	3.94	80,315	61,263	58,650	73.0	95.7
56#	21 Jul	09:18	06:57*	8.31	4.41	34,392	28,878	27,860	83.9	96.5
Totals				46.11	21.68	189,015	159,566	152,580	81.3	95.6

*Consecutive Autosub6000 mission number
†Time vehicle was launched (UTM)
‡Time vehicle secured onboard (UTM). (This was on the next calendar day.)
§Seabed photographic survey phase of mission (h)
|Ship operation time dedicated to Autosub6000 mission (h)
¶Mission 51 was trials mission and thus shorter than all subsequent missions.
#Note M56 lies within PAP central site.

The resampled images were output in GeoTIFF format (http://trac.osgeo.org/geotiff/), with geo-location data in UTM coordinates. For oblique images, the 3-D rotation was applied only to estimate the seabed area observed, no further manipulation was conducted on these images (as it would introduce extreme geometric distortion to water column targets). This manuscript only presents results from the vertical camera.

Removing overlap

Overlap between adjacent pairs of vertical images was determined by geo-location, and removed by cropping half of the overlap from each image (Fig. 4E). Given the vehicle's speed, altitude, and camera acceptance angles, adjacent images were c. 15% overlapped.
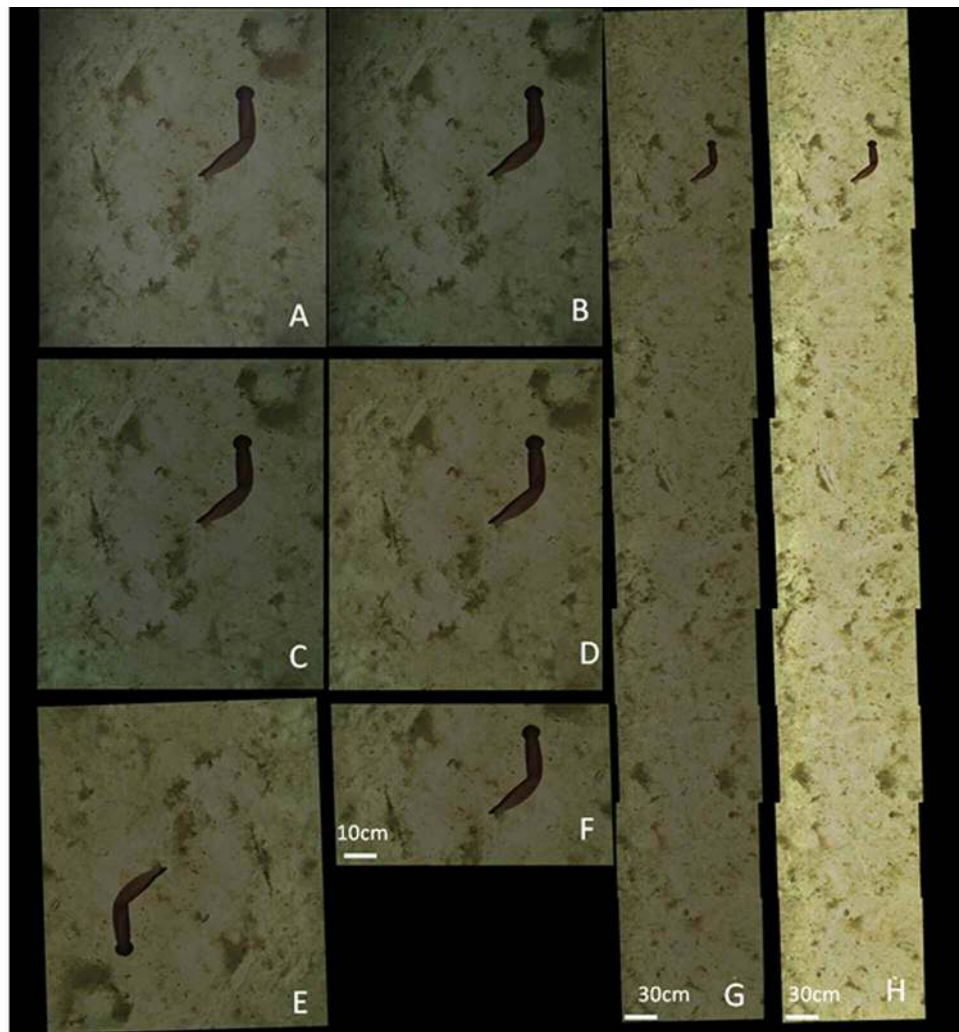
Image tiling

Cropped images were combined in groups of ten to form "tiles." This was achieved using the geo-referencing data associated with each image and the inbuilt Matlab function 'Imfuse' (Fig. 4G) to produce an image tile representing c. 15-20 m^2 of seafloor. Tiles were limited to ten images to allow timely and effective computation, as well as ensuring that the annotation of a single tile could be conducted in an efficient and continuous manner. Note that overlap between adjacent tiles was cropped in the same manner as adjacent images, to prevent double counting and allow a continuous image of the seafloor to be created from the tiles.

Image annotation and data generation

Each tile was opened in Image Pro Plus V7 (Media Cybernetics) and a further brightness histogram correction was applied before annotation to brighten the image (Fig. 4H), allowing organisms to be more visible. Annotation was completed using a custom macro that allowed individual organisms within the tiles to be indicated, categorized according to morphotype, and measured (Fig. 5). The software produced an output database containing the morphotype identification (examples can be found in Fig. 6), a nominal label, length in pixels, and location coordinates of the organism's central point. This pixel-based data were then combined with the embedded geo-location data (GeoTIFF) to convert to 'real-world' units. The seafloor area covered by each tile was calculated, and faunal count data were converted to spatial density units.

Ecological quantification

To assess the method in terms of quantitative ecological parameters, comparisons were made with other techniques employed at the Porcupine Abyssal Plain–Sustained Observatory (PAP-SO): otter trawl (Billett et al. 2001) and off-bottom towed-camera (WASP vehicle). Direct comparison of these methods was complicated by (i) variation in the physical size of the individual sampling unit (e.g., from 0.6 m^2 per WASP photograph, to 20.4 ha by a single trawl), and (ii) the number of individuals identified per sampling unit (e.g., from zero in single WASP photographs and Autosub tiles to 9200 in a single trawl catch). Less readily quantified was variation in the underlying sampled population, for example (iii) inter-annual change in megabenthos density and composition, and (iv) vis-

Fig. 4. Example of image automated processing step outputs from raw image to 10 image tile. A) Raw image, B) Backscatter removed, C) Non-uniform illumination applied, D) Color correction applied, E) Geo-referenced and resized image, F) Correctly positioned and cropped to remove overlap area from image, G)10 image tile, H) Tile, which has been histogram corrected to aid with annotation. Note: the individual used in these images is a *Psychropotes longicauda* as used in the analysis section.

ibility of the fauna (e.g., trawl catches included infaunal organisms which were invisible to photographic methods, and the relative morphological distinctiveness of live in situ fauna versus preserved catch material). To provide some control of factors (i) and (ii), sample pooling and sample-based rarefaction was carried out, and factor (iii) was acknowledged by assessing trawl data in two batches. The dominant form of temporal change in megabenthos communities at the PAP-SO has been referred to as the '*Amperima* Event(s)' (Billett et al. 2010), reflecting apparent boom-bust population dynamics of the small holothurians, *A. rosea*, and other associated community changes. Consequently, we have divided the available trawl catch data into *A. rosea* 'bust' periods 1989-94, 2000, 2004-05, and *A. rosea* 'boom' periods 1996-99, 2002 (see Billett et al. 2010, Fig. 5). WASP data were collected during the RRS *James Cook* 062 cruise during 2011 (Ruhl 2012) (Table 2). Only

WASP transects over level abyssal plane sites were considered for comparisons.

Density estimation

Total megabenthos density was assessed according to the original sampling units (WASP photographs; Autosub6000 tiles and whole trawl catches respectively), and by pooling WASP photographs in to consecutive groups of 3, to approximately match the average area covered by a single Autosub6000 tile. Mean and standard deviation (SD_{ln}) of density per sampling unit were calculated on $\log(x + 1)$ transformed data, to acknowledge the likely aggregated distribution of the megabenthos, and back-transformed to report geometric mean density values (Table 3). A coefficient of variation (CV) in density was calculated for each dataset, based on the log-normal form of $CV = [\exp(SD_{ln}^2) - 1]^{0.5}$ (see e.g., Limpert et al. 2001) and expressed as a percentage. 95% Confidence intervals were

derived for both density and coefficient of variation in each dataset using a bootstrap percentile method from 10,000 re-samplings, implemented using the 'boot' package (Canty and Ripley 2013) in R version 3.0.2 (R Core Team 2013).

To examine potential differences between the methods at the morphotype level, two key taxa were considered: '*Amperima* +,' a complex of the small holothurian genera *Amperima*, *Kolga*, and *Ellipinion*, which are difficult to discriminate in seabed photographs, and the much larger holothurian, *Psychropotes longicauda*. These were chosen due to their presence

Fig. 5. Example of an annotated tile section. L1 to L4 indicate individual organisms that have been identified and measured using the macro tool in ImagePro: L1 sea cucumber *Paroriza* sp.; L2 decapod *Munidopsis* sp.; L3 and L4 anemone *Kadosactis* sp.
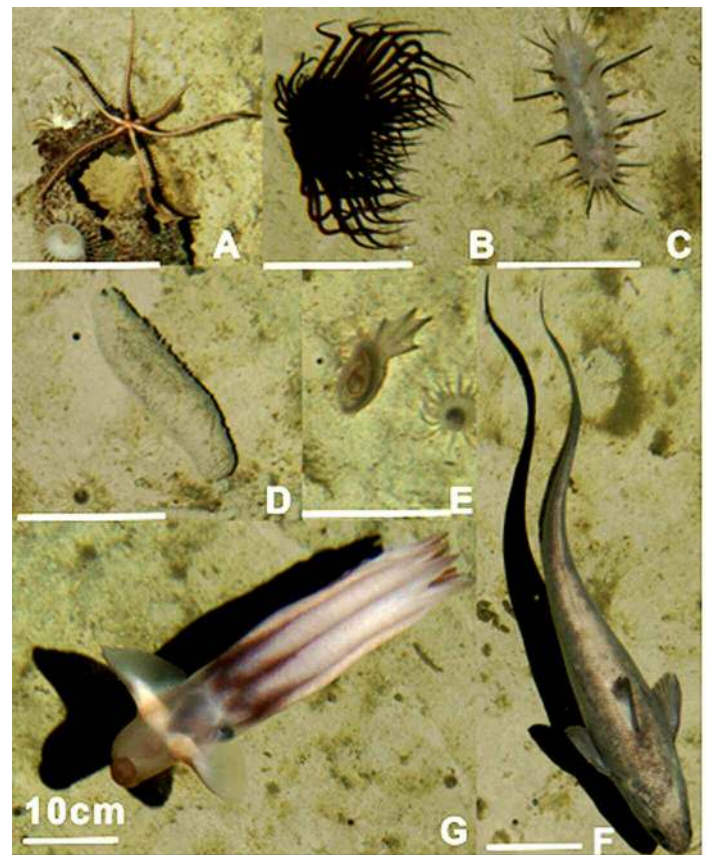
Fig. 6. Example organisms observed during annotation of vertical images. A) *Freyastera* sp. and *Amphianthus* sp., B) *Cerianthid* sp., C) *Oneirophanta* sp., D) *Pseudostichopus villosus*, E) *Amperima* sp. and *Iosactis vagabunda*, (F) *Coryphaenoides armatus*, G) *Grimpoteuthis* sp. Each white scale bar represents 10 cm on the seabed.

Table 2. WASP towed camera system deployment data for RRS *James Cook* cruise 062, Porcupine Abyssal Plain, July/August 2011.

Mission[*]	Date (2011)	Launch[†]	Recover[‡]	Ship time (h)[§]	Survey time (h)[|]	Total nr photos	Nr "useful" photos	% useful of total
PAP C[¶]	27 Jul	16:30	21:55	5.41	0.67	200	85	42.5
H1	05 Aug	12:36	18:47	6.18	1.1	342	217	63.4
F1[¶]	08 Aug	08:11	14:20	6.15	1.08	297	183	61.6
F2[¶]	11 Aug	17:51	23:30	5.65	1.08	323	222	68.7
H2	13 Aug	06:36	12:28	5.86	1.08	337	253	75.1
H3	17 Aug	10:24	13:59	3.58	1.08	180	149	82.8
H4	21 Aug	12:04	18:06	6.03	1.13	228	116	50.9
PAP T[¶]	24 Aug	21:39	04:19	6.66	0.98	307	236	76.9
Total				45.52	8.2	2214	1461	66.0

[*]WASP station identifier.
[†]Time vehicle was launched (UTM).
[‡]Time vehicle was recovered (UTM).
[§]Total ship time required for survey.
[|]Seabed photographic survey phase of mission.
[¶]Level abyssal plan transect used in ecological comparison.
Note. PAP C and M56 are in the same location

Table 3. Comparisons of the Porcupine Abyssal Plain sustained observatory megabenthos density estimates and their precision across techniques.

	Density (ind. ha⁻¹)			Coefficient of variation (%)		
	Geometric mean	95% CI low	95% CI high	Reference sample	95% CI low	95% CI high
WASP photos	3015	2765	3276	27.5	25.0	30.1
WASP 3-photos pooled	2976	2699	3264	17.4	15.2	19.7
Autosub6000-AESA tiles	5170	5100	5241	12.8	12.4	13.2
Trawl catches (*A.* 'bust')	87	73	103	36.8	26.1	43.5
Trawl catches (*A.* 'boom')	264	225	311	45.9	35.2	55.1

CI, confidence interval

in all three data sets allowing a comparison, as well as representing taxa from this study which were "rare and large" (*Psychropotes longicauda*) and a common taxa ('*Amperima +*'), both of which are readily identified.

Diversity estimation

Assessment of megabenthos diversity across techniques was carried out using sample-based rarefaction (Colwell et al. 2012) as implemented with "EstimateS" (version 9.1.0; Colwell et al. 2012). In particular, the 'S(est)' parameter (the expected number of taxa in *t* pooled samples) and Fisher's α diversity index ('α Mean' parameters, e.g., Magurran 2004) were used. For these two parameters, "EstimateS" provides unconditional, analytical estimates of standard deviation (SD), enabling the calculation of a coefficient of variation (CV% = 100 × SD/parameter mean). Following the recommendations of Gotelli and Colwell (2001), comparisons of these parameters were limited across techniques to common expected number of individuals, as given in "EstimateS" by $(t/T) \times N$, where t is the number of sampling units pooled, T is the total number of sampling units, and N is the total number of individuals over all sampling units.

Assessment

Survey efficiency

Use of both the NOC Wide Angle Seabed Photography (WASP) system (Ruhl et al. 2012) and Autosub6000 (present study; Tables 1 and 2) at PAP-SO enables a comparison of photographic survey performance. Autosub6000 has a higher ship-time efficiency, collecting 189,015 images covering some 26 ha in 22 h of ship operation time, representing a survey rate of 1.2 ha h⁻¹. By comparison, WASP covered approximately 0.7 ha in 46 h of ship time (0.015 ha h⁻¹) collecting 2214 images. Considering the generation of quantitative survey data, the effective survey acquisition rate of Autosub6000 could be up-rated to ~2.3 ha h⁻¹ if full battery capacity was employed; the towed camera approach could be up-rated to ~ 0.1 ha h⁻¹ with cabled power and data link to the surface vessel. For additional comparison, the trawl acquisition rate is of the order 0.8 ha h⁻¹, although in terms of 'true quantitative' (i.e., area fully censused) acquisition it is likely to be < 0.08 ha h⁻¹.

The Autosub6000 system returned 96% quantitatively useful images when excluding vehicle turns (Table 1), whereas the WASP system returned only 66% (Table 2). Autosub6000 was programmed to fly at an altitude of 3.2 m above the seabed; however, because of image quality only images in the altitude range 1.9–4.1 proved to be quantitatively useful. The mean altitude of usable images throughout all missions was 3.2 m with a standard deviation (SD) of 0.26 m, indicating a stable operating altitude. By comparison, the mean altitude of all usable images from the WASP vehicle was estimated to be 2.7 m with a SD of 0.82 m. Autosub6000's stability as a camera platform is further illustrated in its corresponding pitch (mean = –1.05°, SD = 1.8°) and roll (mean = 1.22°, SD = 0.95°) statistics. WASP does not carry a pitch and roll sensor, but it is directly impacted by ship's heave, and so is inherently a much less stable camera platform.

Image quality

The automated image processing technique was subjectively assessed by comparing raw images to processed images, and by an assessment of scaling accuracy. Illumination vignetting appeared to be significantly reduced and the usefulness of the image appreciably improved by the illumination correction algorithms (Fig. 4). An improvement in our images might have been achieved with slightly more flash illumination.

Image tiling and quantification

The tiling process was assessed by comparing adjacent images with the corresponding image segment in a tile, to determine if common objects were co-located. The mean displacement of 100 common objects was 4.45 cm (95% Confidence Interval [CI]: 4.14–4.76 cm), with a mean of 150 cm between image centers, giving an along-track (1D) error of 2.97% (95% CI = 2.76–3.17%). A potential source of error in the relative placement of images was the lower frequency of the navigation and altitude data compared with the frame interval rate, i.e., 0.5 Hz versus 1.15 Hz, (or 2 s versus 0.87 s interval). The navigation and altitude data associated with individual photographs were therefore interpolated values and subject to some error. An obvious improvement for the system would be directly matched navigation, altitude, and image acquisition time points. No independent test of

absolute geo-location was undertaken. Combined inertial and Doppler navigation processing was used without implementing any correction for potential drift. Drift is expected to accumulate as 0.1% of distance traveled in higher altitude operations such as bathymetric mapping (McPhail 2009), although this value may increase somewhat in low altitude operations such as photography.

The general success of the tiling process, as assessed by common object displacement, suggested good physical scaling of images to 'real-world' units. This is further supported by the serendipitous observation of two beverage cans on the seabed. In processed tiles, these cans measured 11.7 and 10.9 cm, the true size being 11.2 cm. This limited ground-truthing effort again suggests a 1D error of < 5%.

Ecological quantification

An order of magnitude or greater variation was observed in total megabenthos density estimates between trawls and photographic methods (Table 3). Similarly, trawl estimates had an appreciably lower precision (CV 37% to 46%) than photographic estimates (CV 13% to 28%). Individual WASP photographs provided a lower precision (CV 28%) than individual Autosub6000-based tiles (CV 13%); however, when WASP photos were pooled in consecutive groups of 3 to match the physical scale of tiles, precision was improved (CV 17%) and approximated that of the Autosub6000 method. The precision of Autosub6000 tiles was marginally higher ($P < 0.05$) than the pooled WASP photos. With the Autosub6000 method, it was possible (and will be in subsequent publications) to examine a much greater range of physical scales (i.e., images or tiles per sampling unit).

An order of magnitude variation in '*Amperima* +' density estimates was apparent between trawl *A.* 'bust' (19 ind.ha^{-1}) and *A.* 'boom' periods (190 ind. ha^{-1}) (Fig. 7). All photographic density estimates (confidence limit minimum 388 ind. ha^{-1}) were significantly ($P < 0.05$) higher than the maximum trawl *A.* 'boom' estimate (confidence limit maximum 241 ind. ha^{-1}). There was also significant ($P < 0.05$) variation between WASP (600 ind. ha^{-1}) and Autosub6000 (400 ind. ha^{-1}) density estimates, likely attributable to temporal variation. In contrast, *P. longicauda* exhibited only modest density variation between trawl *A.* 'bust' (4 ind.ha^{-1}) and *A.* 'boom' periods (15 ind.ha^{-1}), with all photographic estimates (16-25 ind.ha^{-1}) broadly comparable to the latter trawl data. This limited variation in *P. longicauda* density is assumed to reflect both a higher trawl fishing efficiency, and a more conservative reproduction strategy of this large species, in comparison to the small taxa that comprise the '*Amperima* +' morphotype.

Over the majority of the range in expected number of individuals observed, the Autosub6000 method produced significantly ($P < 0.05$) higher estimates of morphotype richness than the other techniques (Fig. 8). Compared at common levels of expected number of individuals (Table 4), estimated taxon richness and taxon diversity (Fisher's alpha) were appreciably higher in the Autosub6000 data than the WASP data. However, precision in these estimates was highly consistent between the two photographic methods, with CV ranging
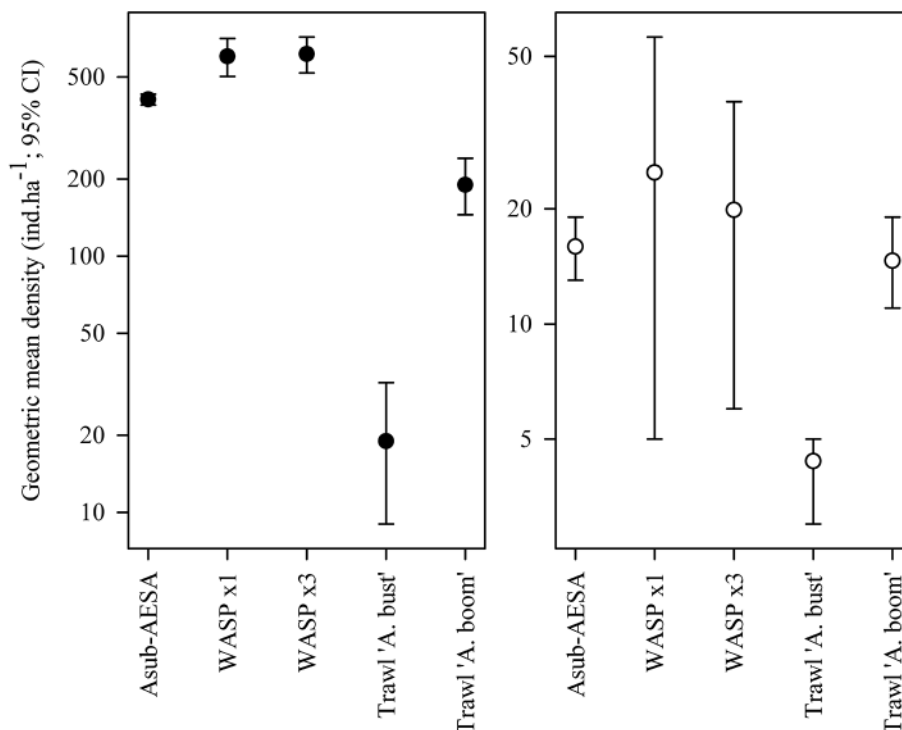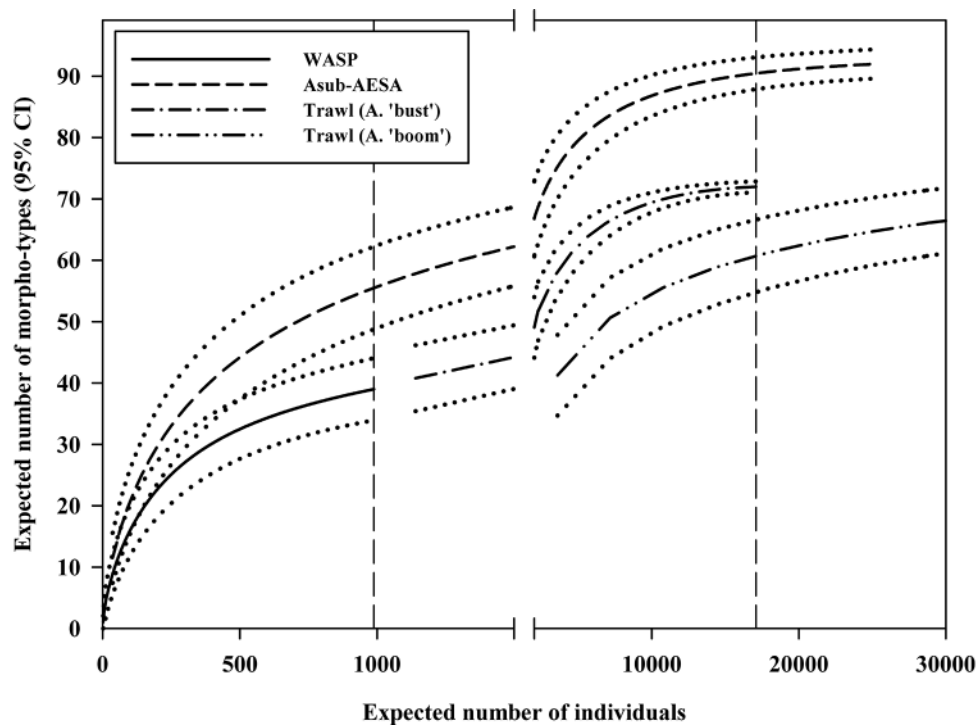

Fig. 7. Comparisons of PAP-SO megabenthos density estimates for key morpho-types (left "*Amperima* + "; right *Psychropotes longicauda*) across techniques.

6.2–6.6% in richness, and 6.9–7.6% in diversity. Similarly, comparisons between the Autosub6000 and trawl data, indicated the former gave appreciably higher values, but there was little variation in precision between techniques, notably in the case of Fisher's α diversity where CV ranged only 3.7–4.4% across the 3 data sets compared. The Autosub6000 method appears to be capable of achieving high accuracy and precision in diversity measures at both smaller and larger physical scales, a combination that neither trawl nor tow camera techniques can accomplish.

Discussion

Through the example of a successful practical survey, and its assessments against alternative techniques the method described appears to permit a broad scale, effective, and efficient investigation of megafaunal ecology at abyssal depths. The method offers an important advance in the ability to study the deep-sea benthos and should facilitate both temporal and spatial studies. The method has a particular application in habitat mapping, where benthic community structures can be compared within a range of habitats as assigned via consideration of abiotic factors, such as rugosity, steepness, and depth derived from acoustic data, as well as features noted from image data. Other applications are in management, and conservation, and may be well suited to surveying frontier areas (e.g., beneath Arctic ice; Dowdeswell et al. 2008) and regions of potential broad-scale human impact (e.g., polymetallic nodule mining; Thiel 2001). AUV opera-

Fig. 8. Comparisons of PAP-SO megabenthos diversity estimates across techniques, as sample-based rarefaction of expected taxon richness. (Vertical dashed lines indicate diversity comparison points detailed in Table 4).

Table 4. Comparisons of the Porcupine Abyssal Plain sustained observatory megabenthos diversity estimates and their precision across techniques.

	Sample units	Individuals	Morphotype richness					Fisher's α diversity		
			S (est)	95% CI low	95% CI high	SD	CV (%)	Mean	SD	CV (%)
Autosub-AESA tiles	110	984	55.5	48.7	62.2	3.44	6.2	12.6	0.86	6.9
WASP photos	726	988	39.0	33.9	44.1	2.59	6.6	8.1	0.62	7.6
Autosub-AESA tiles	1910	17093	90.5	87.9	93.1	1.33	1.5	12.6	0.47	3.7
Trawl catches (*A.* 'bust')	15	17093	72.0	71.1	72.9	0.45	0.6	9.6	0.40	4.2
Trawl catches (*A.* 'boom')	5	17942	61.3	55.4	67.2	3.00	4.9	8.0	0.35	4.4

S(est), expected morphotype richness; CI, confidence interval; SD, standard deviation; CV, coefficient of variation

tions under ice do require special considerations for deployment, operational communications, and recovery. However, examples of AUV deployments through breaks in ice and away from the edge of ice sheets have shown that under ice research is tractable. Special consideration is also warranted for handling intervention/abort scenarios, including if/how mechanisms such as drop weights or acoustic and satellite beacons are used. Here we used an automated abort drop weight (with optional manual control via acoustic communications), as well as an Argos satellite transponder, which activates upon surfacing, giving an independent means to locate the vehicle. But, we typically did not communicate with the vehicle except to track its position while working on other tasks in its vicinity.

In the present survey, landscape-scale megabenthos and environmental data have been effectively generated. In doing so, a near-continuous 1D visual image of the abyssal seafloor that extends for some 160 km, encompassing approximately 26 h, has been generated. The accuracy of the combined inertial and DVL navigation of the Autosub6000 vehicle and its altitude sensor data allowed areas of contiguous photograph overlap to be removed to within c. 3% accuracy (1D), allowing a continuous image to be formed that simplifies subsequent analysis and interpretation.

The choice of methods depends, of course, on analytical requirements. For example, some data sets have limited navigational input or have a requirement to mosaic images in two dimensions. Here we have restricted our approach to mosaicking and tiling in one dimension, but many issues apply in both cases. Previously developed mosaicking techniques made key advances as detailed below, but many such tools had limitations for high-throughput processing. Pizarro and Singh (2003) produced mosaics from ROV images, where location data were not available, using feature detection and blending. Although effective, this would not be efficient over large areas, with small errors magnifying over the transect length, particularly in areas of relatively featureless seabed. Singh et al. (2004) described a spatial mosaicking method that worked well for small areas and allowed individual strips to be automatically created. However, for the highest resolution images to be achieved, these strips had to be created image by image. Such manual mosaic creation has been effective in some studies (e.g., Marsh et al. 2013), but is not practical for surveys consisting of tens of thousands of images, or more.

Singh et al (2004) also described a Fourier transformation technique, which was able to resolve rotations of 0.3° and 0.44% change in scaling, and appeared to be successful for images with a large amount of overlap. The scheme described here uses a three-axis rotation and translation to the seabed, allowing for perspective correction. The individual pixel georeferencing allows mosaicking to occur even if gaps occur between images. Mosaicking using both feature matching and geo-referencing methods was achieved by Escartin et al. (2008) using 20,823 images obtained by the ARGO II towed camera

system. Each image was assigned the camera's geographic location and rotated solely on heading, as pitch and roll were thought to be stable enough to be discounted. An issue with their method was that some features appeared to be masked in overlapping frames, as a result of blending (removing the visible border between single images). Barreyre et al. (2012) created mosaics of the Lucky Strike hydrothermal vent site, from 56,000 images acquired 1996-2009 using ROVs (Prados et al. 2012). Primary navigation was provided by USBL and matching of features between images was necessary to further tune the navigation. This was followed by image blending. As expertise related to image processing expands, and tools are brought together in new ways, we expect that high-throughput mosaic creation methods will improve and effectively include blending.

Although complicated by temporal variation and other factors, the comparative density results suggested substantial undersampling of the megabenthos by trawling of about an order of magnitude (minimum photographic confidence limit 2700 ind.ha^{-1} versus maximum trawl confidence limit 300 ind. ha^{-1}). In addition, the '*Amperima* +' and *P. longicauda* comparisons suggested a potential body size–related variation in trawl fishing efficiency. Using the Autosub6000 data as the denominator, '*Amperima* +' trawl fishing efficiency was 5% to 46% and *P. longicauda* trawl fishing efficiency was 28% to 92%, depending on bust or boom conditions. Similar conclusions were previously reported by Bett et al. (2001) in a comparison of PAP-SO trawl data with time-lapse camera data.

Whereas there are no concurrent WASP or trawl data with which to compare the Autosub6000 method results, the total megabenthos density estimate (5200 ind.ha^{-1}) was of the same order as those derived by detailed analyses of time-lapse photographs (Bett et al. 2001) during the 1997-2000 *Amperima* boom period (5700-8400 ind.ha^{-1}). Though not conclusive, this would suggest the Autosub6000 method was as effective and potentially accurate with respect to even the smaller fractions of the megabenthos. Further, its apparent high precision (CV 13%) promises good sensitivity in the detection of change (spatial and temporal) in megabenthos communities.

Autosub6000 data were also shown to have a higher diversity estimate than the other methods. It was not entirely clear why the WASP diversity estimate should be lower than that of the Autosub6000. It is possible that this is partly due to a change in the type of camera used, leading to images of a different resolution and different illumination characteristics. Other possibilities include temporal variation in density and/or dominance levels. This effect is well illustrated in the comparison of trawl *A.* 'bust' and *A.* 'boom' periods (Fig. 8). During the *A.* 'bust' period, the median rank-1-dominance (Magurran 2004) was 29% (22% to 32% interquartile range) but was substantially higher at 51% (39% to 67% IQR) during the *A.* 'boom' period. This change in dominance is reflected in the slope of the corresponding rarefaction curves. Rank-1-dominance varied only modestly between the WASP (53%)

and Autosub6000 (47%) data sets, and was occupied by the same taxon in both cases (*Iosactis vagabunda*). Greater variation was, however, apparent in the '*Amperima +*' morphotype, the rank-2 taxon (20%) in the WASP data, having a density of 600 ind. ha^{-1}, switching to the rank-3 taxon (8%) with a density of 400 ind. ha^{-1} in the Autosub6000 data. It may also be that the image correction (e.g., illumination, color, etc.) used in the Autosub6000 method led to improved specimen detection, for example more reliable recording of the presence and identity of small, low contrast specimens, such as ophiuriods.

Again there are no concurrent data with which to make a conclusive comparison with the Autosub6000 method results. Nevertheless, that the richness and diversity estimates consistently exceeded those of the other methods tested suggests that it is highly effective. With a good precision (CV < 10%) of richness and diversity estimation achieved in a sample size as low as 30-40 tiles, the method promises very good sensitivity in the detection of change (spatial and temporal) in megabenthos communities.

The practicalities of bulk image storage and processing are important to consider. In the present study, the most effective data retrieval was to remove the hard-drive from the AUV and transfer images from them via cable onto a multi-disk mass storage server. Working with raw images, geo-referenced images, tiled-images, and annotated tiles multiplies the data volume in non-trivial ways, though not all of these data need be retained in the longer term. The time to process and annotate mass-collected images can also be substantial and must be considered during survey design. However, despite some limitations, it is expected that this method will enable a step-change in megabenthos ecological data quantity and quality at the PAP-SO site.

Summary

In summary, the Autosub6000-AESA methodology, described and assessed above, offers very significant advantages over the alternative techniques tested. (i) The use of a stable autonomous imaging platform greatly enhances effective survey acquisition per hour of committed shiptime where the AUV system offers 20-100 fold improvement over the towed camera. (ii) In terms of quantifying megabenthos density, the Autosub6000 techniques appears to offer a 10-50 fold improvement in accuracy over the trawl, i.e., there is a greater than one order-of-magnitude under-sampling by the trawl. This low fishing efficiency is likely to be nonrandom across taxa and body sizes, such that trawl samples are both quantitatively and qualitatively inferior to the photographic data. However, it must be noted that trawls do have the clear advantage of allowing physical specimen collections and thus achieve a higher level of taxonomic resolution. (iii) The Autosub6000 tiles provided a two-fold improvement in density estimate precision when compared with individual WASP images, however this is most likely a spatial-scale effect (i.e., aggregate patch size) rather than method related. (iv) Comparisons of taxon richness and diversity across techniques are complex and encompass a number of uncontrolled factors. It is, nevertheless, clear that the Autosub6000 method uniformly produced 30% to 60% higher estimates than either WASP (towed camera) or trawl data for the same sample size (as number of individuals). (v) Trawls may destroy and break up soft-bodied or fragile animals and miss smaller organisms entirely, which can be viewed and successfully counted using off-bottom photo surveys

Comments and recommendations

Through the enhanced spatial resolution achieved by this method, we expect the data obtained to be particularly valuable in revealing relationships between the megabenthos and various environmental parameters, such as proximity to topography and patches of phytodetritus. A key limitation of the method is that only those megabenthos visible at the sediment surface are censused, although some data on the mega-infauna may be derived from analyses of lebensspurren (Bell et al. 2013).

The Autosub6000 camera system described here has already been successfully employed in a combined geophysical and photographic survey of an inshore (100 m water depth) marine-protected area (Wynn et al. 2014). The system is currently employed in further continental shelf operations, and will soon be deployed on missions concerned with deep-sea resource exploitation (seafloor mining; oil and gas). There will be further development of the instrumentation and technique through the Autosub Long Range (LR) vehicle (Wynn et al. 2014), which has substantially enhanced range and endurance, including a hibernation mode. It will be possible to run repeat surveys (e.g., monthly) at the PAP-SO site during a single AutosubLR deployment, with the vehicle hibernating on the seabed between surveys. This capability will give unprecedented insights into benthic temporal variability in the deep sea, and an efficient high-throughput methodology to process and analyze images will be key.

Acknowledgments

References

Bell, J. B, D. O. B Jones, and C. H. S. Alt. 2013. Lebensspuren of the bathyal Mid-Atlantic Ridge. Deep-Sea Res. II 98:341-351 [doi:10.1016/j.dsr2.2012.09.004].

Bett, B. J., A. L. Rice, and M. H. Thurston. 1995. A quantitative photographic survey of "spoke-burrow" type lebensspuren on the Cape Verde Abyssal Plain. Int. Rev. Hydrobio. Berlin 80:153-170 [doi:10.1002/iroh.19950800204].

———, M. G. Malzone, B. E. Narayanaswamy, and B. D. Wigham. 2001. Temporal variability in phytodetritus and megabenthic activity at the seabed in the deep northeast Atlantic. Prog. Oceanogr. 50:349-368 [doi:10.1016/S0079-6611(01)00066-0].

Barreyre, T., T. Escartin, R. Garcia, M. Cannat, E. Mittelstaest, and R. Prados. 2012. Structure, temporal evolution, and heat flux estimates from the Lucky Strike deep-sea hydrothermal fiels derived from seafloor image mosaics. Geochem. Geophys. Geosyst. 13 [doi:10.1029/2011GC003990].

Billett, D. S. M., B. J. Bett, A. L. Rice, M. L. Thurston, J. Galéron, M. Sibuet, and G. A. Wolff. 2001. Long-term change in the megabenthos of the Porcupine Abyssal Plain (NE Atlantic). Prog. Oceanogr. 20:325-348 [doi:10.1016/S0079-6611(01)00060-X].

———, ———, W. D. K. Reid, B. Boorman, and I. G. Priede. 2010. Long-term change in the abyssal NE Atlantic: The "Amperima Event" revisited. Deep-Sea Res. II 57:1406-1417 [doi:10.1016/j.dsr2.2009.02.001].

Canty, A., and B. Ripley. 2013. boot: Bootstrap R (S-Plus) functions. R package vers. 1.3-9.

Chiang, J. Y., and Y. C. Chen. 2012. Underwater image enhancement by wavelength compensation and dehazing. IEEE Trans. Image Process. 21:1755-1769 [doi:10.1109/TIP.2011.2179666].

Chase, J. M., and T. M. Knight. 2013. Scale-dependent effect sizes of ecological drivers on biodiversity: why standardised sampling is not enough. Ecol. Lett. 16:17-26 [doi:10.1111/ele.12112].

Colwell, R. K., A. Chao, N. J. Gotelli, S.-Y. Lin, C. X. Mao, R. L. Chazdon, and J. T. Longino. 2012. Models and estimators linking individual-based and sample-based rarefaction, extrapolation, and comparison of assemblages. Plant Ecol. 5:3-21 [doi:10.1093/jpe/rtr044].

Dowdeswell, J. A., and others. 2008. Autonomous underwater vehicles (AUVs) and investigations of the ice-ocean interface: deploying the Autosub AUV in Antarctic and Arctic waters. J. Glaciol. 54:661-672 [doi:10.3189/002214308786570773].

Escartín, J., and others. 2008. Globally aligned photomosaic of the Lucky Strike hydrothermal vent field (Mid-Atlantic Ridge, 37°18.5′ N): Release of georeferenced data, mosaic construction, and viewing software. Geochem. Geophys. Geosyst. 9 [doi:10.1029/2008GC002204].

Forman, R. T. T. 1983. An ecology of the landscape. BioScience 3:535.

———, and M. Godron. 1986. Landscape ecology. Wiley.

Glover, A. G., and others. 2010. Temporal change in deep-sea benthic ecosystems: a review of the evidence from recent time-series studies. Adv. Mar. Biol. 58:1-95.

Gotelli, N. J., and R. K. Colwell. 2001. Quantifying biodiversity: procedures and pitfalls in the measurements and comparison of species richness. Eco. Lett. 4:379-391 [doi:10.1046/j.1461-0248.2001.00230.x].

Hartman, S. E., K. E. Larkin, R. S. Lampitt, M. Lankhorst, and S. J. Hydes. 2010. Seasonal and inter-annual biogeochemical variations in the Porcupine Abyssal Plain 2003–2005 associated with winter mixing and surface circulation. Deep-Sea Res. II 57:1303-1312 [doi:10.1016/j.dsr2.2010.01.007].

———, and others. 2012. The Porcupine Abyssal Plain fixed-point sustained observatory (PAP-SO): variations and trends from the Northeast Atlantic fixed-point time-series. ICES J. Mar. Sci. 69:776-783 [doi:10.1093/icesjms/fss077].

Haedrich, R. L., and N. R. Merrett. 1988. Summary atlas of deep living demersal fishes in the North Atlantic Basin. J. Nat. Hist. 22:1325-1362 [doi:10.1080/00222938800770811].

Heger, A., E. N. Ieno, N. J. King, K. J. Morris, P. M. Bagley, and I. G. Priede. 2008. Deep-sea pelagic bioluminescence over the Mid-Atlantic Ridge. Deep-Sea Res. II 55:126-136.

Jones, D. O. B., B. J. Bett, and P. A. Tyler. 2007. Megabenthic ecology of the deep Faroe-Shetland Channel: a photographic study. Deep-Sea Res. I 54:1111-1128 [doi:10.1016/j.dsr.2007.04.001].

———, ———, R. B. Wynn, and D. G. Masson. 2009. The use of towed camera platforms in deep-water science. Int. J. Soc. Underw. Technol. 28 41-50 [doi:10.3723/ut.28.041].

Kalogeropoulou, V., B. J. Bett, N. Lampadariou, M. Arbizu, and A. Vanreusel. 2010. Temporal changes (1989-1999) in deep-sea metazoan meiofauna assemblages on the Porcupine Abyssal Plain, NE Atlantic. Deep-Sea Res. II 15:1383-1395 [doi:10.1016/j.dsr2.2009.02.002].

Limpert, E., W. A. Stahel, and M. Abbit. 2001. Log-normal distributions across the sciences: Keys and clues. Bioscience 5:341-352 [doi:10.1641/0006-3568(2001)051[0341:LNDATS]2.0.CO;2].

McPhail, S. D. 2009. Autosub6000: a deep diving long range AUV. J. Bionic Eng. 6:55-62 [doi:10.1016/S1672-6529(08)60095-5].

———, and M. Pebody. 2009. Range-only positioning of a deep-diving autonomous underwater vehicle from a surface ship. IEEE J. Oceanic Eng. 34:669-667 [doi:10.1109/JOE.2009.2030223].

Magurran. A. E. 2004. Measuring biological diversity. Blackwell Publishing.

Marsh, L., J. T. Copley, V. A. I. Huvenne, and P. A. Tyler. 2013. Getting the bigger picture: Using precision Remotely Oper-

ated Vehicle (ROV) videography to acquire high-definition mosaic images of newly discovered hydrothermal vents in the Southern Ocean. Deep-Sea Res. II 92:124-135 [doi:10.1016/j.dsr2.2013.02.007].

Morris, K. J., P. A. Tyler, B. Murton, and A. D. Rogers. 2012. Lower bathyal and abyssal distribution of coral in the axial volcanic ridge of the Mid-Atlantic Ridge at 45° N. Deep-Sea Res. I 62:32-39 [doi:10.1016/j.dsr.2011.11.009].

———, ———, D. G. Masson, V. A. I. Huvenne, and A. D. Rogers. 2013. Distribution of cold-water corals in the Whittard Canyon, NE Atlantic Ocean. Deep-Sea Res. II 92:136-144 [doi:10.1016/j.dsr2.2013.03.036].

Pizarro, O., and H. Singh. 2003. Towards large area mosaicing for underwater scientific applications. IEEE J. Oceanic Eng. 28:651-672 [doi:10.1109/JOE.2003.819154].

Prados, R., R. Garcia, N. Gracias, J. Escartin, and L. Neumann. 2012. A novel blending technique for underwater gigamosaicing. IEEE J. Oceanic Eng. 99:626-644 [doi:10.1109/JOE.2012.2204152].

R Core Team. 2013. R: A language and environment for statistical computing. R Foundation for Statistical Computing. <http://www.R-project.org/>

Ramirez-Llodra, E., and others. 2011. Man and the last great wilderness: Human impact on the deep sea. PLOS One. 6:e22588 [doi:10.1371/journal.pone.0022588].

Rice, A. L. 1990. RRS Discovery Cruise 185, 18 August–17 September 1989. Abyssal benthic biology at the European Community Station (48, 50′N 16, 30′W). Institute of Oceanographic Sciences Deacon Laboratory.

———, R. G. Aldred, E. Darlington, and R. A. Wild. 1982. The quantitative estimation of the deep-sea megabenthos: a new approach to an old problem. Oceanol. Acta 5:63-72.

Ruhl, H. A. 2012. RRS James Cook Cruise 62, 24 Jul–29 Aug 2011. Porcupine Abyssal Plain—sustained observatory research. National Oceanography Centre Cruise Report, No. 12.

———. 2013. RRS Discovery Cruise 377 and 378, 05–27 Jul 2012, Southampton to Southampton. Autonomous ecological surveying of the abyss: understanding mesoscale spatial heterogeneity at the Porcupine Abyssal Plain: National Oceanography Centre.

———, and others. 2011. Societal need for improved understanding of climate change, anthropogenic impacts, and geo-hazard warning drive development of ocean observatories in European Seas. Prog. Oceanogr. 91:1-33 [doi:10.1016/j.pocean.2011.05.001].

Singh, H., J. Howland, and O. Pizarro. 2004. Large area photomosaicking underwater. IEEE J. Oceanic Eng. 29:872-886 [doi:10.1109/JOE.2004.831619].

Smith, K. L., H. A. Ruhl, M. Kahru, C. L. Huffard, and A. D. Sherman. 2013. Deep ocean communities impacted by changing climate over 24 y in the abyssal northeast Pacific Ocean. Proc. Nat. Acad. Sci. 110:19838-19841 [doi:10.1073/pnas.1315447110].

Soto, E. H., G. L. J. Paterson, D. S. M. Billett, L. E. Hawkins, J. Galéron, and M. Sibuet. 2010. Temporal variability in polychaete assemblages of the abyssal NE Atlantic Ocean. Deep-Sea Res. II 57:1267-1428 [doi:10.1016/j.dsr2.2009.02.003].

Stoner, A. W., C. H. Ryer, S. J. Parker, P. J. Auster, and W. W. Wakefield. 2008. Evaluating the role of fish behavior in surveys conducted with underwater vehicles. Can. J. Fish. Aquat. Sci. 65:1230-1243 [doi:10.1139/F08-032].

Svoboda, A. 1985. Diver-operated cameras and their marine-biological uses. *In* J. D. George, G. I. Lythgoe, and J. N. Lythgoe (eds.), Underwater photography and television for scientists. Clarendon Press.

Tyler, P. A. 2003. Ecosystems of the deep oceans. Elsevier.

Thiel, H. 2001. Evaluation of the environmental consequences of polymetallic nodule mining based on the results of the TUSCH Research Association. Deep-Sea Res. II 48:3433-3452 [doi:10.1016/S0967-0645(01)00051-0].

Wakefield, W. W., and A. Genin. 1987. The use of a Canadian (perspective) grid in deep sea photography. Deep Sea Res. 34:469-478 [doi:10.1016/0198-0149(87)90148-8].

Wheeler, A. J., and others. 2013. Moytirra: Discovery of the first known deep—sea hydrothermal vent field on the slow spreading Mid-Atlantic Ridge north of the Azores. Geochem. Geophys. Geosyst. 14:4170-4184 [doi:10.1002/ggge.20243].

Wynn, R., and others. 2014. Autonomous Underwater Vehicles (AUVs): their past, present and future contributions to the advancement of marine geosciences. Mar. Geol. 352:451-468.